IEEE Access
Multidisciplinary | Rapid Review | Open Access Journal

Received August 20, 2020, accepted October 23, 2020, date of publication October 27, 2020, date of current version November 10, 2020.

Digital Object Identifier 10.1109/ACCESS.2020.3034151

A Fast Sand-Dust Image Enhancement Algorithm by Blue Channel Compensation and Guided Image Filtering

YAQIAO CHENG[1,2], ZHENHONG JIA[1,2], HUICHENG LAI[1,2], JIE YANG[3], (Member, IEEE), AND NIKOLA K. KASABOV[4], (Fellow, IEEE)

[1]College of Information Science and Engineering, Xinjiang University, Urumqi 830046, China
[2]Key Laboratory of Signal Detection and Processing, Xinjiang Uygur Autonomous Region, Xinjiang University, Urumqi 830046, China
[3]Institute of Image Processing and Pattern Recognition, Shanghai Jiao Tong University, Shanghai 200400, China
[4]Knowledge Engineering and Discovery Research Institute, Auckland University of Technology, Auckland 1020, New Zealand

Corresponding author: Zhenhong Jia (jzhh@xju.edu.cn)

This work was supported in part by the National Science Foundation of China under Grant U1803261, and in part by the International Science and Technology Cooperation Project of the Ministry of Education of the People's Republic of China under Grant DICE 2016–2196.

ABSTRACT The images captured in sand-dust weather have the characteristics of color deviation and low visibility, which seriously affect computer vision systems. To solve the above problems, we propose a fast and effective algorithm to enhance the images captured in sand-dust weather conditions. First, we compensate for the loss value in the blue channel. Then, white balancing technology is used to correct the color of the sand-dust-degraded image. Finally, guided image filtering is used to enhance the image contrast and edge accuracy, and an adaptive method is used to calculate the magnification factor of the detail layer to enhance the image detail information. The experimental results on a large number of sand-dust-degraded images show that the method can effectively recover the fading characteristics of sand-dust-degraded images in a short time and improve the clarity of the images. Experimental results via qualitative and quantitative evaluations demonstrate that the proposed method can significantly improve the images captured during sand-dust weather conditions, and the results are better than those of other methods.

INDEX TERMS Sand-dust-degraded image, blue channel compensation, color correction, guided image filtering.

I. INTRODUCTION

The images captured in sand-dust weather have the characteristics of low contrast, color deviation and blur, which seriously affect the clarity of the image. The main reason for this phenomenon is the scattering and absorption of light by sand-dust particles. Therefore, the sand-dust-degraded images have directly reduced the processing capacity of monitoring systems, automated driving and remote sensing systems.

To improve the processing ability of computer vision systems in sand-dust environments, researchers have proposed some visibility restoration algorithms, as discussed in Section II. This prior work to improve the clarity of sand-dust images can be divided into three classes.

Current sand-dust-degraded image enhancement algorithms can resolve color deviations, enhance image contrast and improve image clarity, but some problems remain. First, when using the current color correction technology to process the sand-dust-degraded images, blue artifacts appear in the images and reduce the image quality. Second, the current sand-dust-degraded image enhancement algorithms have a high time complexity.

Therefore, in this study, we propose a fast and effective method that can improve the contrast and chroma of the sand-dust-degraded images. The following are the main steps in the proposed method. First, a blue channel recovery algorithm is proposed that can recover the blue channel by compensating for the lost value. Second, guided image filtering is used to enhance the image contrast and edge accuracy, and an adaptive method is proposed to calculate the magnification coefficient for the detail layer to enhance the image detail information.

The associate editor coordinating the review of this manuscript and approving it for publication was Madhu S. Nair.

The experimental results obtained through qualitative and quantitative evaluations show that this method can effectively improve the images captured under sand-dust weather conditions in a short period of time and produce better results than other methods.

II. RELATED WORK

The existing methods to improve the clarity of sand-dust images can be grouped in several classes. The first class of approaches employs an atmospheric scattering model [1], [2], a Laplacian distribution model [3] and a Retinex model [4]. The algorithms in [1], [2] use a geometric framework to analyze the chromatic effects of atmospheric scattering. Huang *et al*. [3] presented a novel Laplacian-based visibility restoration approach to effectively solve inadequate haze thickness estimation and alleviate color cast problems. Based on the robust Retinex model, an optimization function proposed in [4] includes new regularization terms of illumination and reflectivity. First, it constrains the segmented smoothness of the lighting and then uses fidelity to enhance the details of the image. These algorithms have good performance in defogging or low-light image enhancement; however, the effect of the processed sand-dust degraded image is not ideal.

A second class of approaches consists of image processing methods. These methods combine color correction and contrast enhancement to enhance the sand-dust images. For example, adaptive contrast enhancement [5]–[7] has been employed for this purpose. Wang *et al.* [8] introduced the fractional differential theory algorithm. Yan *et al*. [9] proposed a sand-dust image enhancement method combining the spatial domain and the transform domain. In this method, PAL fuzzy enhancement is first applied to the image, then the adaptive equalization algorithm is used to improve the image contrast, and finally POSHE is used to enhance the image detail information. Fu *et al*. [10] fused color correction, gamma correction and three weight map processing to enhance the definition of sand-dust-degraded images. Wang *et al*. [11] transformed the sand-dust-degraded image into the CIELAB space, processed the color component with color correction and contrast stretching, and processed the brightness component with local Laplace filtering. The employed algorithm in [12] can rapidly process sand-dust-degraded images by using the optimized fuzzy enhancement operator. Yang *et al*. [13] proposed an optical compensation method to correct the sand-dust image color cast, and used the linear constraint of the Gaussian function to optimize the transmission. These methods can solve the sand-dust image color deviation and improve the contrast, but the processed image will contain blue artifacts, which affects the image quality.

Recently, several algorithms that specifically restore sand-dust images based on the dark channel prior (DCP) have been introduced. The DCP was first proposed by He *et al*. [14] to recover the images captured in dehazing by estimating the ambient light and its transmission. Mixed spectrum analysis technology and DCP technology were used in [15] to correct the image color deviation and to perform defogging, respectively, to enhance the visibility of defogging in bad weather. Jin-Song *et al.* [16] proposed a new adaptive image sharpening method based on DCP method. Huang *et al*. [17] combined the DCP, color correction and visibility restoration to enhance image quality. Huang *et al*. [18] proposed a new method combining thickness estimation, color analysis and visibility restoration by improving the algorithm employed in [17]. Yu *et al*. [19] proposed an information loss constraint algorithm based on DCP technology. The algorithms in [20], [21] estimated the transmission by calculating the difference between the observed intensity and ambient light and were combined with color correction to enhance the sand-dust-degraded images. Shi *et al*. [22] presented a halo-reduced DCP algorithm, which mainly includes three modules: color correction, defogging and contrast enhancement. Very recently, [23] introduced a sand-dust image restoration method based on reversing the blue channel prior. A blue channel and fusion algorithm [24] recovered images by using blue channel technology, and then the fusion algorithm enhanced the contrast, chroma and edge intensity of the images. Although the improved DCP algorithm can restore the image clarity of sand-dust images, the sky region of the processed image is distorted.

III. PROPOSED METHOD

In this study, we propose a visibility restoration algorithm based on blue channel compensation and guided image filtering that is used to enhance the degraded images captured under sand-dust weather conditions. The proposed method consists of two parts: white balancing based on blue channel compensation and guided image filtering. First, to restore the fading characteristics of the degraded images and effectively resolve the blue artifacts, we compensate the lost blue value and apply white balancing processing to the compensated image. Second, guided image filtering is used to improve the contrast and edge accuracy of the sand-dust-degraded image, and an adaptive method is used to calculate the magnification factor of the detail layer to enhance the detail information of the degraded image.

A. WHITE BALANCING BASED ON BLUE CHANNEL COMPENSATION

The purpose of white balancing is to improve the image quality, but the processed sand-dust image will have blue artifacts, which reduces the image quality. Therefore, we propose a white balancing color correction method based on blue channel compensation. The purpose is to restore the blue channel by compensating the lost blue value. This method can solve the color cast of sand-dust-degraded images and effectively eliminate blue artifacts.

1) BLUE CHANNEL COMPENSATION

In sand-dust environment conditions, most of the blue light is scattered and absorbed, which causes the images captured

FIGURE 1. (a) Input sand-dust image. The remaining five images are the restoration results of (b) white balancing, (c) gray world, (d) the OCM, (e) color balance, and (f) our white balancing.

in sand-dust weather to have an overall yellow appearance and color distortion. To correct the yellow appearance, we apply white balancing, gray world, the optical compensation method (OCM) [13] and color balance [25] processing to the sand-dust-degraded images. The results are shown in Fig. 1.

Fig. 1 (b)-(c) reveals that the traditional white balancing and gray world algorithms have poor performance when dealing with sand-dust-degraded images, and blue artifacts appear in degraded images; therefore, these methods cannot effectively solve the color cast problem. Fig. 1 (d) shows that the processed image still has blue artifacts, and a layer of mist appears on the surface of the processed image. The compensation method is proposed in the algorithm implemented in [25]. The processing result obtained by using this algorithm to compensate the blue channel is shown in Fig. 1 (e). In this figure, the processed sand-dust-degraded image appears light blue overall, blue artifacts appeared on the edges of the vehicles and white objects on the ground, and the overall image is dark. Therefore, we improve the algorithm presented in [25] and propose a blue channel compensation method for sand-dust-degraded images.

We compensate the missing blue channel through the following three observations.

First, most of the blue light in the sand-dust weather conditions is scattered and absorbed; therefore, an image captured in sand-dust weather appears yellow overall. Hence, if we want to better handle the sand-dust images, we need to restore the blue channel.

Second, the gray world assumes that the average reflection of the natural scenery of the light is the same in general, and all channels have the same mean value in a zero-depth scene; therefore, we can use this hypothesis to restore the blue channel by compensating for the lost value.

Third, in sand-dust-degraded image processing, we assume that the mean values of the green channel and the red channel are unchanged to carry out blue channel recovery experiments. Through these experiments, we find that the effect of blue channel recovery is better if the mean value of the green channel is unchanged. Therefore, we ensure that the green channel's mean is unchanged to compensate the blue channel.

Through the above three observations, we obtain the blue channel compensation formula as follows:

$$I_{\mathrm{bc}}(\mathrm{x}) = I_{\mathrm{b}}(\mathrm{x}) + \frac{\bar{I}_g - \bar{I}_b}{\bar{I}_r + \bar{I}_g + \bar{I}_b} * I_g(x) \tag{1}$$

where I_{bc} is the compensated blue channel; I_g and I_{b} are the green channel and blue channel of image I, respectively;$\bar{I}_r$, $\bar{I}_g$ and $\bar{I}_b$ are the mean values of the red channel, green channel and blue channel in image I, respectively; and x represents the pixel position.

As shown in Fig. 1 (f), the improved blue channel compensated white balancing algorithm can solve the problem of sand-dust color deviation, can effectively eliminate the blue artifacts in sand-dust images, and can improve the quality of sand-dust images.

2) WHITE BALANCING

Color deviation still existed after blue channel compensation, so the white balancing algorithm was selected to correct the color of the compensated image. Most of the white balancing methods generally estimate the color of the light source through specific assumptions and then divide each color channel by the corresponding normalized light source intensity to achieve color constancy. Among those methods, the gray-world algorithm [26] assumes that the average value of RGB components of an image with color change tends to the same gray value. Therefore, the color distribution of the light source can be estimated by averaging each channel independently. The Retinex theory [27] assumes that the maximum response of each channel is caused by the white block, and the maximum response in each color channel can be used to estimate the color of the light source. The gray edge of [28] assumes that the average edge difference in the scene is achromatic and calculates the scene illumination color by applying the Minkowski p-norm to the derivative structure of the image channels instead of the zero order pixel structure. This method has been proven to obtain results that are comparable to the most advanced color constancy methods even though its calculation is simple [25].

After a comprehensive comparison, we used Robust-AWB [29] to correct the color deviation of the sand-dust image.

FIGURE 2. **(a) Input sand-dust image and its license plate image. (b) Our white balancing enhanced sand-dust image and its license plate image. The remaining two images are the result of processing (b) using the methods of (c) guided Image filtering[30] and (d) the proposed guided Image filtering.**

The algorithm used the gray color points in the extracted image to estimate the color temperature. The color temperature of the light source was estimated by the small color difference between the gray color point and the gray color point under different color temperatures.

B. GUIDED IMAGE FILTERING

The key assumption of the guided image filtering is that the filter output q is a linear transform of a guided image I in a window w_k centered at pixel k [30]. The linear model is as follows:

$$q_i = a_k I_i + b_k, \quad \forall i \in w_k \tag{2}$$

where a_k and b_k are constants in a window w_k and i and k are indices. This linear model only ensures that q has an edge when I has an edge, because $\nabla \mathrm{q} = \overline{a} \nabla I$. a_k and b_k are obtained by minimizing the cost function, and the cost function is as follows:

$$E(a_k, b_k) = \sum\nolimits_{i \in w_k} ((a_k I_i + b_k - p_i)^2 + \varepsilon a_k^2) \tag{3}$$

where p is the input image, and ε is a regularization parameter preventing a_k from being too large. Through the linear ridge regression model (3), a_k and b_k can be obtained as follows:

$$a_k = \frac{\frac{1}{|\omega|} \sum_{i \in w_k} I_i p_i - \mu_k \overline{p}_k}{\sigma_k^2 + \varepsilon} \tag{4}$$

$$b_k = \overline{p}_k - a_k \mu_k \tag{5}$$

where μ_k and σ_k^2 are the mean and variance of I in w_k,respectively, and $|\omega|$ is the number of pixels in w_k.

The filter output image q_i can be calculated by taking the obtained coefficients a_k and b_k into equation (2). It can be written as follows:

$$q_i = \overline{a}_i I_i + \overline{b}_i \tag{6}$$

where $\overline{a}_i = \frac{1}{|\omega|} \sum_{k \in w_k} a_k$ and $\overline{b}_i = \frac{1}{|\omega|} \sum_{k \in w_k} b_k$.

As shown in Fig. 2 (c), the sand-dust-degraded image after using guided image filtering has noise because the magnification of the detail layer is generally a fixed value, which magnifies the details and amplifies the noise. Therefore, we improve the magnification of the detail layer and propose an adaptive magnification calculation method.

The following is our main method to obtain the adaptive magnification. The input image p is given, and its edge-preserving smoothed output is used as a base layer q. The difference between the input image and the base layer is the detail layer [30], which can be written as follows:

$$d = p - q \tag{7}$$

where d is the detail layer, p is the input image, and q is the base layer. The detail information can be improved by increasing the magnification factor of the details, and the formula is as follows:

$$d_m = \beta d = \beta(\mathrm{p} - \mathrm{q}) \tag{8}$$

where β is the magnification, and d_m is the boosted detail layer. The output image is a combination of the boosted detail layer d_m and the base layer q, and the formula is as follows:

$$p = d_m + q \tag{9}$$

The gradient relation between p and q is $\nabla \mathrm{q} = \overline{a} \nabla p$. We considered that the gradient relation of the base layer

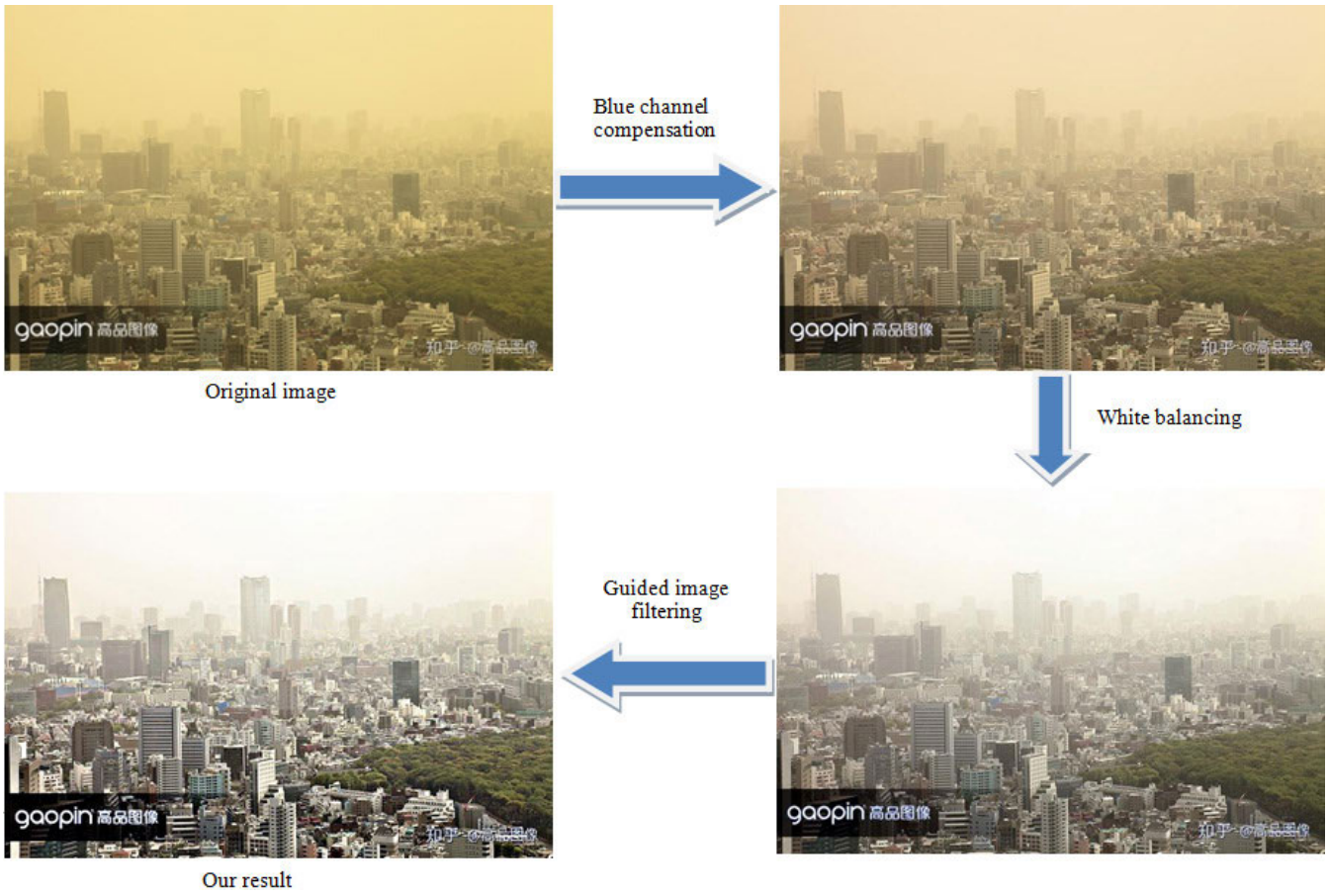

FIGURE 3. The framework of the proposed algorithm.

should be equal to the detail layer; otherwise, the noise will increase. Therefore, we obtain the following equation.

$$d_m = \beta(\mathrm{p} - \mathrm{q}) = \beta(\mathrm{p} - \overline{a}\mathrm{p} - \overline{\mathrm{b}}) \tag{10}$$

$$\nabla d_m = \nabla q = \overline{a}\nabla p \tag{11}$$

By solving the above equation, we can obtain the adaptive amplification coefficient β. The results are as follows:

$$\beta = \frac{\overline{a}}{1 - \overline{a}} \tag{12}$$

where $\overline{a}_i = \frac{1}{|\omega|} \sum_{k \in w_k} a_k$.

To better illustrate the effectiveness of the algorithm, we perform color correction on the sand-dust-degraded images, and then conduct guided image filtering [30] and modified guided image filtering on the processed images. The results are shown in Fig. 2. By comparing Fig. 2 (c) and (d), we found that the modified guided image filter can effectively eliminate the noise in the image and enhance the contrast, edge accuracy and detail information of the sand-dust-degraded image. As shown Fig. 2, we found that the proposed algorithm can effectively enhance the clarity of the sand-dust-degraded image. The proposed algorithm can also enhance the license plate information in sand-dust environment conditions and provide services for license plate recognition under surveillance video.

As mentioned, the proposed algorithm framework is shown in Fig. 3. First, we performed blue channel compensation processing on the sand-dust-degraded image, and effectively restored the lost value in the blue channel. Second, we performed white balancing processing on the blue channel compensated image, and this process can effectively eliminate the color cast of the sand-dust-degraded image. Third, we used guided image filtering, which aims to enhance the contrast and edge accuracy of the degraded image, and then we used an adaptive method to calculate the amplification factor of the detail layer to enhance the image detail information.

C. EXPERIMENTAL RESULTS

In this section, we conducted a qualitative evaluation and a quantitative evaluation on the processed sand-dust-degraded images to verify the effectiveness of the proposed algorithms. We compared the most representative methods described in Alameen [12], Li *et al.* [4], Fu *et al.* [10], Yang *et al.* [13], Shi *et al.* [22] and Cheng *et al.* [24]. First, we performed a qualitative visual comparison. Second, we performed a quantitative no-reference quality assessment with 300 sand-dust images. Third, we conducted a time complexity comparison.

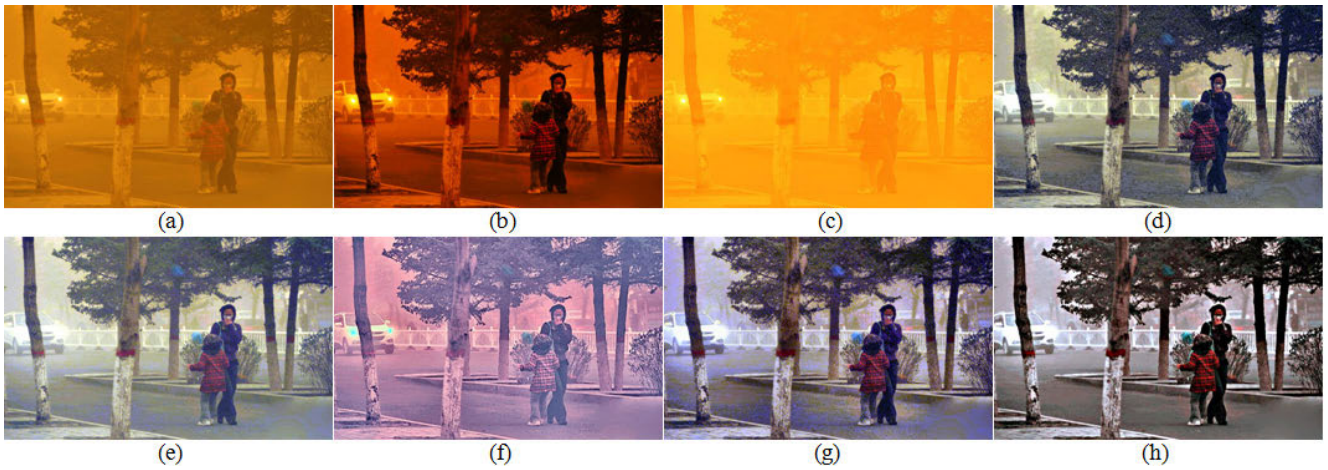

FIGURE 4. (a) Input sand-dust image. The remaining seven images are the restoration results generated by the methods of (b) Alameen [12], (c) Li *et al.* [4], (d) Fu *et al.* [10], (e) Yang *et al.* [13], (f) Shi *et al.* [22], (g) Cheng *et al.* [24] and (h) the proposed method.

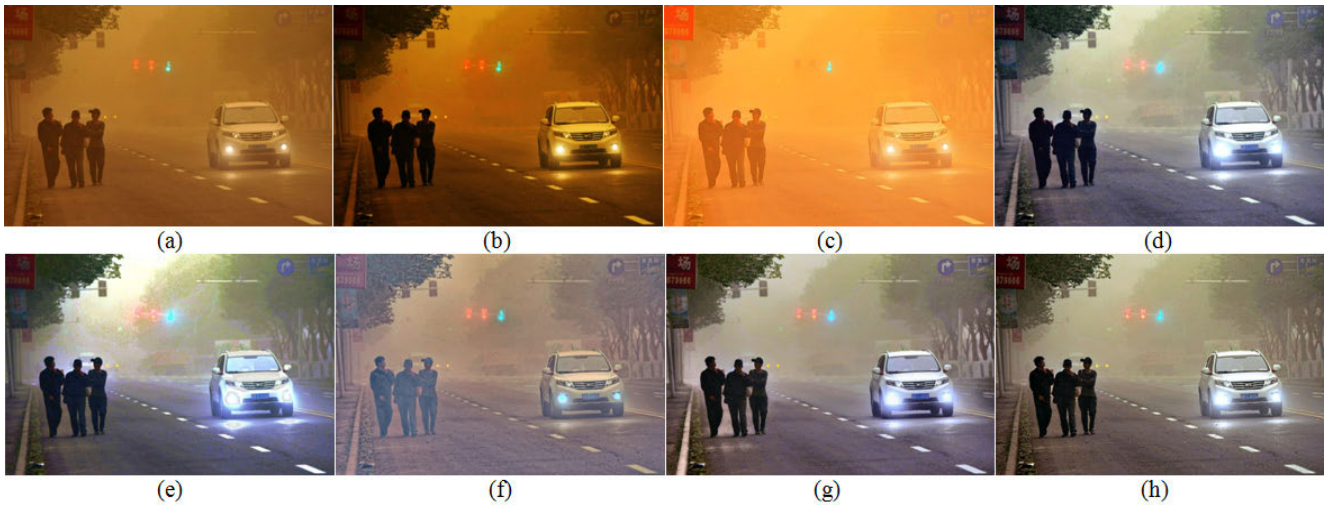

FIGURE 5. (a) Input sand-dust image. The remaining seven images are the restoration results generated by the methods of (b) Alameen [12], (c) Li *et al.* [4], (d) Fu *et al.* [10], (e) Yang *et al.* [13], (f) Shi *et al.* [22], (g) Cheng *et al.* [24] and (h) the proposed method.

In this study, all compared approaches were implemented by using MATLAB 2016a on an Intel Core i5-3320 CPU 2.60 GHz processor with 6 GB of RAM, running a Windows 7 operating system.

D. QUALITATIVE EVALUATION

To better illustrate the effectiveness of the algorithms, all of the tested images were derived from the real sand-dust environment. We used the approaches of Alameen [12], Li *et al.* [4], Fu *et al.* [10], Yang *et al.* [13], Shi *et al.* [22], Cheng *et al.* [24] and the proposed method to process the images, and the results are shown in Figs. 4–7.

As shown in Figs. 4(a)-7(a), the original sand-dust-degraded images have the characteristics of color deviation, low contrast and blur, which seriously affected the clarity of the images. As shown in Figs. 4(b)-(c) to 7(b)-(c), the sand-dust-degraded images processed by the methods of Alameen [12] and Li *et al.* [4] have serious color deviations, and an orange or red appearance, which seriously affect the image quality. The surfaces of the processed images still have the characteristics of blur and low contrast, which did not enhance the sharpness of the images. As shown in Figs. 4(d)-7(d), using the method of Fu *et al.* [10] to process the sand-dust images can resolve the color deviation and improve the clarity of the image, but the processed images are dark, which affects the visual perception. In Figs. 4(d)-5(d), the processed images showed blue artifacts and local color deviation. As shown in Figs. 4(e)-5(e), the images processed by the method of Yang *et al.* [13] have severe blue artifacts, and the light areas in the images are distorted. Furthermore, a large area of noise appeared in the sky area at the top of the image in Fig. 7(e), and the brightness of the image was low. As shown in Figs. 4(f)-7(f), the sharpness of the

FIGURE 6. (a) Input sand-dust image. The remaining seven images are the restoration results generated by the methods of (b) Alameen [12], (c) Li *et al.* [4], (d) Fu *et al.* [10], (e) Yang *et al.* [13], (f) Shi *et al.* [22], (g) Cheng *et al.* [24] and (h) the proposed method.

FIGURE 7. (a) Input sand-dust image. The remaining seven images are the restoration results generated by the methods of (b) Alameen [12], (c) Li *et al.* [4], (d) Fu *et al.* [10], (e) Yang *et al.* [13], (f) Shi *et al.* [22], (g) Cheng *et al.* [24] and (h) the proposed method.

images processed by the method of Shi *et al.* [22] was not sufficiently restored, and the color deviation was severe. A red appearance, noise and distortion can be observed in the processed image shown in Fig. 4(f). The sand-dust-degraded image processed by the method of Cheng *et al.* [24] exhibited blue artifacts, as shown in Fig. 4(g). Figs. 4(h)-7(h) present the sand-dust-degraded images processed by the proposed method, illustrating that the above problems are effectively solved and that the clarity of the images is improved.

In this study, 20 subjects were selected for a qualitative evaluation of the non-reference quality, and 19 of them considered image (h) to be superior to the other images.

E. QUANTITATIVE EVALUATION

The non-reference method was used to evaluate the sand-dust-degraded images objectively because of the lack of sand-dust-free reference images. Three kinds of non-reference evaluation metrics, namely, e, $\bar{r}$ [31] and the natural image quality evaluator (NIQE) [32], were used to evaluate the sand-dust images. e and $\bar{r}$ metrics represent the ratio of new visible edges in sand-dust-free images and the quality of contrast restoration in sand-dust-free images, respectively. The higher the evaluation values of e and $\bar{r}$ are, the better the restoration effect. NIQE uses spatial domain natural scene statistics to evaluate the sand-dust-degraded images. The smaller the evaluation value of NIQE is, the better the recovery effect.

Evaluation metrics e, $\bar{r}$ and NIQE were used to measure the processing results of Figs. 4-7, and the results are shown in Table 1-3, respectively. To illustrate the effectiveness of the algorithms better, the methods of Alameen [12], Li *et al.* [4], Fu *et al.* [10], Yang *et al.* [13], Shi *et al.* [22], Cheng *et al.* [24] and the proposed algorithm were used to measure 300 images obtained in the real

TABLE 1. Sand-dust images of Figs. 4-7 restoration evaluation based on the e metric. A larger metric is better.

	Original	Alameen [12]	Li *et al.*[4]	Fu *et al.*[10]	Yang *et al.*[13]	Shi *et al.*[22]	Cheng *et al.*[24]	Our method
Fig. 4	---	1.9947	-0.9331	3.2800	2.5830	2.6610	3.2949	3.3293
Fig. 5	---	8.7818	-0.8320	22.7783	16.7979	25.9096	25.7341	25.4933
Fig. 6	---	0.6066	-0.2820	3.6339	1.1695	4.6673	4.7108	4.9214
Fig. 7	---	0.5616	-0.3979	1.6362	1.6374	1.6933	1.6996	1.7260
Average	---	2.9862	-0.6113	7.8321	5.5470	8.7328	8.8599	8.8675

TABLE 2. Sand-dust images of Figs. 4-7 restoration evaluation based on the $\bar{r}$ metric. A larger metric is better.

	Original	Alameen [12]	Li *et al.*[4]	Fu *et al.*[10]	Yang *et al.*[13]	Shi *et al.*[22]	Cheng *et al.*[24]	Our method
Fig. 4	---	2.1731	0.5196	4.0709	2.6792	4.0342	4.1530	4.2532
Fig. 5	---	1.3986	1.5260	2.9309	2.5319	4.4884	3.1384	3.2990
Fig. 6	---	1.7438	1.0484	2.9737	1.7347	4.9430	3.0872	3.5254
Fig. 7	---	1.6065	1.3840	2.4882	1.9653	3.8105	2.4661	3.0791
Average	---	1.7305	1.1195	3.1159	2.2278	4.3190	3.2112	3.5392

TABLE 3. Sand-dust images of Figs. 4-7 restoration evaluation based on the ***NIQE*** metric. A small metric is better.

	Original	Alameen [12]	Li *et al.*[4]	Fu *et al.*[10]	Yang *et al.*[13]	Shi *et al.*[22]	Cheng *et al.*[24]	Our method
Fig. 4	3.0492	3.1461	4.7007	3.1937	2.9938	3.7172	2.8492	2.7209
Fig. 5	7.0908	6.7545	4.7047	6.1618	5.9778	5.6109	5.0948	4.5868
Fig. 6	3.6192	3.2173	4.8264	3.1686	3.2165	3.1036	2.9293	2.8159
Fig. 7	3.7491	2.9869	3.7067	3.0087	2.9850	3.7120	2.9967	2.8704
Average	4.3771	4.0262	4.4846	3.8832	3.7933	4.0359	3.4675	3.2485

TABLE 4. Comparison of average restoration acquired by the e, $\bar{r}$ and ***NIQE*** metrics for ***300*** sand-dust images.

	Original	Alameen [12]	Li et al.[4]	Fu et al.[10]	Yang et al.[13]	Shi et al.[22]	Cheng et al.[24]	Our method
e	---	2.9156	-0.6756	7.3346	5.7555	7.9172	8.2572	8.2657
$\bar{r}$	---	1.7054	1.8441	3.0164	2.3556	4.0952	3.1252	3.4925
NIQE	5.8829	4.2657	4.7633	4.0512	3.9832	4.1578	3.8381	3.5179

sand-dust environment, and the results are shown in Table 4. As shown in Table 1, *e* was taken as the evaluation metric, and the results of the proposed algorithm were better than those of the other algorithms, which shows that our algorithm can effectively recover the number of visible edges of the sand-dust-degraded image.

As shown in Table 2, $\bar{r}$ was taken as the evaluation metric, and the restoration results of the algorithm in [22] were better than the proposed algorithm because the algorithm in [22] used DCP technology to improve the contrast of the image and then CLAHE to enhance the contrast of the L component in the LAB space; however this approach led to increased time complexity and reduced the image processing efficiency.

As shown in Table 3, NIQE was taken as the evaluation metric, and the results of the proposed algorithm were smaller than those of the algorithms, which showed that the image processed by the proposed algorithm was better than that of the other algorithms and improved the quality of the sand-dust-degraded image well. The processing data presented in Table 4 further demonstrates the superiority of the proposed algorithm.

F. TIME COMPLEXITY

For a 900 * 555 image, the running times of the methods of Alameen [12], Li *et al.* [4], Fu *et al.* [10], Yang *et al.* [13], Shi *et al.* [22], Cheng *et al.* [24] and the proposed algorithm are compared, and the results are shown in Table 5. The proposed algorithm takes 1.41 seconds to process the image, which is much shorter than the time required by our previous algorithm [24]. Compared with the time taken by the algorithms in [4], [10], [13] and [22], our algorithm has obvious advantages in terms of time complexity. The algorithm in [12] takes 1.37 seconds to process the image, which is slightly shorter than the proposed algorithm, but the proposed algorithm shows superiority in the other parameters evaluated. To better illustrate the effectiveness of the results,

TABLE 5. Time complexity of each method.

Method	Time(s)	Average(s)
Alameen [12]	1.37	1.43
Li *et al*. [4]	36.96	40.22
Fu *et al*. [10]	3.51	3.60
Yang *et al*. [13]	2.89	2.94
Shi *et al*. [22]	21.11	21.68
Cheng *et al*. [24]	8.35	8.42
Our method	1.41	1.46

we tested the time complexity of 25 sand-dust images and averaged the results as shown in Table 5. The data shows that the time complexity of the proposed algorithm is superior to that of the other algorithms.

IV. CONCLUSION

In this study, we propose a novel visibility restoration method based on blue channel compensation and guided image filtering that is used to recover sand-dust-degraded images. First, we used blue channel compensation technology to recover the lost value in the blue channel. Next, we used the white balancing technology to solve the color deviation problem and combined it with blue channel compensation technology to effectively resolve the appearance of blue artifacts. Finally, guided image filtering was used to enhance the image contrast and edge accuracy, and an adaptive method was used to calculate the magnification factor of the detail layer to enhance the image detail information. The experimental results show that the proposed method based on blue channel compensation and guided image filtering is significantly better than other algorithms.

REFERENCES

[1] S. K. Nayar and S. G. Narasimhan, "Vision in bad weather," in *Proc. 7th IEEE Int. Conf. Comput. Vis. (ICCV)*, Kerkyra, Greece, Sep. 1999, pp. 820–827.
[2] S. G. Narasimhan and S. K. Nayar, "Chromatic framework for vision in bad weather," in *Proc. CVPR, IEEE Conf. Comput. Vis. Pattern Recognit.*, Hilton Head Island, SC, USA, Jun. 2000, pp. 598–605.
[3] S.-C. Huang, J.-H. Ye, and B.-H. Chen, "An advanced single-image visibility restoration algorithm for real-world hazy scenes," *IEEE Trans. Ind. Electron.*, vol. 62, no. 5, pp. 2962–2972, May 2015.
[4] M. Li, J. Liu, W. Yang, X. Sun, and Z. Guo, "Structure-revealing low-light image enhancement via robust Retinex model," *IEEE Trans. Image Process.*, vol. 27, no. 6, pp. 2828–2841, Jun. 2018.
[5] Y. Y. Schechner and Y. Averbuch, "Regularized image recovery in scattering media," *IEEE Trans. Pattern Anal. Mach. Intell.*, vol. 29, no. 9, pp. 1655–1660, Sep. 2007.
[6] M. Alruwaili and L. Gupta, "A statistical adaptive algorithm for dust image enhancement and restoration," in *Proc. IEEE Int. Conf. Electro/Inf. Technol.*, Dekalb, IL, USA, May 2015, pp. 286–289.
[7] R. T. Tan, "Visibility in bad weather from a single image," in *Proc. 26th IEEE Conf. Comput. Vis. Pattern Recognit.*, Anchorage, AK, USA, Jun. 2008, pp. 1–8.
[8] X. Wang, Y. Ju, and T. Gao, "Enhancement techniques for degraded traffic video images under sandstorms based on fractional differential," *Qinghua Daxue Xuebao/J. Tsinghua Univ.*, vol. 52, pp. 61–64 and 68, Oct. 2012.
[9] T. Yan, L. J. Wang, and J. X. Wang, "Method to enhance degraded image in dust environment," *J. Softw.*, vol. 9, no. 10, pp. 2672–2677, Oct. 2014.
[10] X. Fu, Y. Huang, D. Zeng, X.-P. Zhang, and X. Ding, "A fusion-based enhancing approach for single sandstorm image," in *Proc. 16th IEEE Int. Workshop Multimedia Signal Process. (MMSP)*, Jakarta, Indonesia, Sep. 2014, pp. 1–5.
[11] J. Wang, Y. Pang, Y. He, and C. Liu, "Enhancement for dust-sand storm images," in *Proc. 22nd Int. Conf. Multimedia Modeling*, Miami, FL, USA, Jan. 2016, pp. 842–849.
[12] Z. Alameen, "Visibility enhancement for images captured in dusty weather via tuned tri-threshold fuzzy intensification operators," *Int. J. Intell. Syst. Appl.*, vol. 8, no. 8, pp. 10–17, 2016.
[13] Y. Yang, C. Zhang, L. Liu, G. Chen, and H. Yue, "Visibility restoration of single image captured in dust and haze weather conditions," *Multidimensional Syst. Signal Process.*, vol. 31, pp. 619–633, Aug. 2019.
[14] K. He, J. Sun, and X. Tang, "Single image haze removal using dark channel prior," *IEEE Trans. Pattern Anal. Mach. Intell.*, vol. 33, no. 12, pp. 2341–2353, Dec. 2011.
[15] B.-H. Chen and S.-C. Huang, "Improved visibility of single hazy images captured in inclement weather conditions," in *Proc. 15th IEEE Int. Symp. Multimedia*, Anaheim, CA, USA, Dec. 2013, pp. 267–270.
[16] W. Jin-Song, A. Chao, and Y. Peng, "Method and application of image clearness in bad weather," in *Proc. Int. Conf. Commun. Mobile Comput.*, Shenzhen, China, Dec. 2010, pp. 40–44.
[17] S.-C. Huang, B.-H. Chen, and Y.-J. Cheng, "An efficient visibility enhancement algorithm for road scenes captured by intelligent transportation systems," *IEEE Trans. Intell. Transp. Syst.*, vol. 15, no. 5, pp. 2321–2332, Oct. 2014.
[18] S.-C. Huang, B.-H. Chen, and W.-J. Wang, "Visibility restoration of single hazy images captured in real-world weather conditions," *IEEE Trans. Circuits Syst. Video Technol.*, vol. 24, no. 10, pp. 1814–1824, Oct. 2014.
[19] S. Yu, H. Zhu, J. Wang, Z. Fu, S. Xue, and H. Shi, "Single sand-dust image restoration using information loss constraint," *J. Mod. Opt.*, vol. 63, no. 21, pp. 2121–2130, May 2016.
[20] Y.-T. Peng and P. C. Cosman, "Single image restoration using scene ambient light differential," in *Proc. 23rd IEEE Int. Conf. Image Process.*, Phoenix, AZ, USA, Sep. 2016, pp. 1953–1957.
[21] Y.-T. Peng, K. Cao, and P. C. Cosman, "Generalization of the dark channel prior for single image restoration," *IEEE Trans. Image Process.*, vol. 27, no. 6, pp. 2856–2868, Jun. 2018.
[22] Z. H. Shi, Y. N. Feng, M. H. Zhao, E. H. Zhang, and L. F. He, "Let you see in sand dust weather: A method based on halo-reduced dark channel prior dehazing for sand-dust image enhancement," *IEEE Access*, vol. 7, pp. 116722–116733, 2019.
[23] G. Gao, H. Lai, Z. Jia, Y. Liu, and Y. Wang, "Sand-dust image restoration based on reversing the blue channel prior," *IEEE Photon. J.*, vol. 12, no. 2, Apr. 2020, Art. no. 3900216, doi: 10.1109/JPHOT.2020.2975833.
[24] Y. Cheng, Z. Jia, H. Lai, J. Yang, and N. K. Kasabov, "Blue channel and fusion for sandstorm image enhancement," *IEEE Access*, vol. 8, pp. 66931–66940, 2020.
[25] C. O. Ancuti, C. Ancuti, C. De Vleeschouwer, and P. Bekaert, "Color balance and fusion for underwater image enhancement," *IEEE Trans. Image Process.*, vol. 27, no. 1, pp. 379–393, Jan. 2018.
[26] G. Buchsbaum, "A spatial processor model for object colour perception," *J. Franklin Inst.*, vol. 310, no. 1, pp. 1–26, Jul. 1980.
[27] E. H. Land, "The Retinex theory of color vision," *Sci. Amer.*, vol. 237, no. 6, pp. 108–128, Dec. 1977.
[28] J. van de Weijer, T. Gevers, and A. Gijsenij, "Edge-based color constancy," *IEEE Trans. Image Process.*, vol. 16, no. 9, pp. 2207–2214, Sep. 2007.
[29] J.-Y. Huo, Y.-L. Chang, J. Wang, and X.-X. Wei, "Robust automatic white balance algorithm using gray color points in images," *IEEE Trans. Consum. Electron.*, vol. 52, no. 2, pp. 541–546, May 2006.
[30] K. He, J. Sun, and X. Tang, "Guided image filtering," *IEEE Trans. Pattern Anal. Mach. Intell.*, vol. 35, no. 6, pp. 1397–1409, Jun. 2013.
[31] N. Hautiere, J. P. Tarel, D. Aubert, and E. Dumont, "Blind contrast enhancement assessment by gradient ratioing at visible edges," *Image Anal. Stereol.*, vol. 27, no. 2, pp. 87–95, 2008.
[32] A. Mittal, R. Soundararajan, and A. C. Bovik, "Making a 'completely blind' image quality analyzer," *IEEE Signal Process. Lett*, vol. 20, no. 3, pp. 209–212, Mar. 2013.

YAQIAO CHENG received the B.S. degree from the Department of Information Science and Engineering, Xinjiang University, Urumqi, China, in 2017. He is currently pursuing the master's degree with the School of Information Science and Engineering, Xinjiang University. His research interests include clarity of video and images in sand-dust conditions.

ZHENHONG JIA received the B.S. degree from Beijing Normal University, Beijing, China, in 1985, and the M.S. and Ph.D. degrees from Shanghai Jiao Tong University, Shanghai, China, in 1987 and 1995, respectively. He is currently a Professor with the Autonomous University Key Laboratory of Signal and Information Processing Laboratory, Xinjiang University, China. His research interests include digital image processing, photoelectric information detection, and sensor.

HUICHENG LAI received the B.E. and M.S. degrees from Xinjiang University, in 1986 and 1990, respectively. He is currently a Professor with Xinjiang University, China. His current research interests include image processing, image recognition, image enhancement, image restoration, and communications technology.

JIE YANG (Member, IEEE) received the Ph.D. degree from the Department of Computer Science, Hamburg University, Germany, in 1994. He is currently a Professor with the Institute of Image Processing and Pattern Recognition, Shanghai Jiao Tong University, China. His major research interests include object detection and recognition, data fusion and data mining, and medical image processing.

NIKOLA K. KASABOV (Fellow, IEEE) received the M.S. degree in computing and electrical engineering and the Ph.D. degree in mathematical sciences from the Technical University of Sofia, Sofia, Bulgaria, in 1971 and 1975, respectively. He is currently the Director and the Founder of the Knowledge Engineering and Discovery Research Institute and a Professor of knowledge engineering with the School of Computing and Mathematical Sciences, Auckland University of Technology, Auckland, New Zealand. His major research interests include information science, computational intelligence, neural networks, bioinformatics, and neuroinformatic.